

3. ENVIRONMENTAL STATUS 2024

In this section, the status of the environment as of end of 2024 is listed and illustrated.

Table 3.1: Number of objects orbiting Earth. Other: IGO, GHO, HAO, UFO, ESO.

	PL	PF	PD	PM	RB	RF	RD	RM	UI	Total
LEO	11682	5126	111	217	949	3747	32	521	112	22497
GEO	800	35	2	8	67	0	0	0	33	945
EGO	543	791	2	50	201	88	4	5	2207	3891
GTO	49	29	1	10	229	203	10	49	666	1246
NSO	290	0	0	1	99	0	0	2	47	439
MEO	74	1	5	50	27	122	1	4	565	849
LMO	85	135	5	44	257	749	21	210	1051	2557
MGO	72	75	1	3	175	2714	5	0	1520	4565
HEO	29	190	0	2	55	143	0	0	1624	2043
Other	48	12	0	4	7	1	0	0	142	214
Total	13672	6394	127	389	2066	7767	73	791	7967	39246

Table 3.2: Absolute and equivalent number of objects intersecting with the protected regions.

	PL	PF	PD	PM	RB	RF	RD	RM	UI	Total
both (abs)	17	43	1	1	73	126	0	16	381	658
LEO_{IADC} (abs)	11830	5327	117	272	1474	4756	63	780	2052	26671
LEO_{IADC} (eqv)	11713	5213	114	228	1001	3920	37	555	268	23048
GEO_{IADC} (abs)	972	995	5	50	307	1031	2	17	4320	7699
GEO_{IADC} (eqv)	845	172	2	18	105	46	0	1	249	1439
none (abs)	887	115	6	68	358	2106	8	10	1976	5534

Table 3.3: Mass in tons orbiting Earth. Objects of unknown mass do not contribute to the figures presented. Other: IGO, GHO, HAO, UFO, ESO.

	PL	PF	PD	PM	RB	RF	RD	RM	UI	Total
LEO	5205.6	0.0	0.0	4.2	1445.1	0.0	0.0	6.5	0.0	6661.3
GEO	2652.3	0.0	0.0	1.0	138.4	0.0	0.0	0.0	0.0	2791.7
EGL	996.5	0.0	0.0	5.1	386.1	0.0	0.0	0.3	0.0	1388.1
GTO	92.3	0.0	0.0	1.0	512.8	0.0	0.0	21.9	0.0	628.0
NSO	375.0	0.0	0.0	0.4	227.0	0.0	0.0	0.0	0.0	602.4
MEO	82.3	0.0	0.0	0.4	46.5	0.0	0.0	4.2	0.0	133.4
LMO	79.6	0.0	0.0	6.9	520.4	0.0	0.0	86.6	4.0	697.4
MGO	100.7	0.0	0.0	1.9	291.7	0.0	0.0	0.0	0.0	394.3
HEO	49.5	0.0	0.0	0.1	141.2	0.0	0.0	0.0	0.0	190.7
Other	73.7	0.0	0.0	0.1	17.9	0.0	0.0	0.0	0.0	91.6
Total	9707.4	0.0	0.0	20.9	3727.1	0.0	0.0	119.6	4.0	13579.0

Table 3.4: Absolute and equivalent mass in tons intersecting with the protected regions.

	PL	PF	PD	PM	RB	RF	RD	RM	UI	Total
both (abs)	15.9	0.0	0.0	0.1	166.2	0.0	0.0	4.5	0.0	186.6
LEO_{IADC} (abs)	5385.2	0.0	0.0	12.1	2591.5	0.0	0.0	115.0	4.0	8107.8
LEO_{IADC} (eqv)	5232.6	0.0	0.0	5.8	1524.3	0.0	0.0	17.2	0.7	6780.7
GEO_{IADC} (abs)	2977.3	0.0	0.0	6.4	605.9	0.0	0.0	4.6	0.0	3594.2
GEO_{IADC} (eqv)	2755.6	0.0	0.0	2.2	208.9	0.0	0.0	0.4	0.0	2967.0
none (abs)	1360.8	0.0	0.0	2.6	695.9	0.0	0.0	4.4	0.0	2063.7

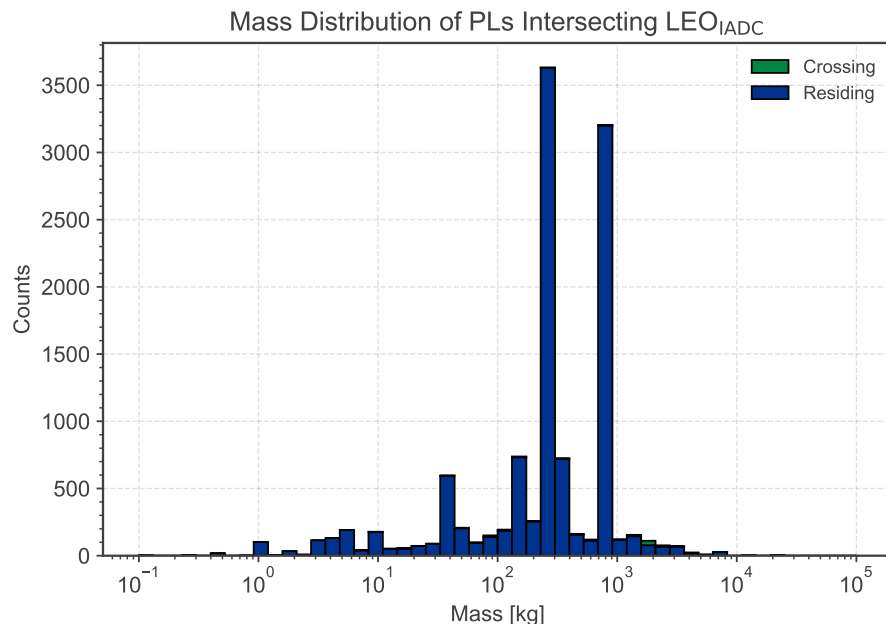
Table 3.5: Area in m^2 orbiting Earth. Objects of unknown area do not contribute to the figures presented. Other: IGO, GHO, HAO, UFO, ESO.

	PL	PF	PD	PM	RB	RF	RD	RM	UI	Total
LEO	165542.6	0.0	0.0	39.1	10923.3	1.3	0.0	258.2	0.0	176764.6
GEO	25770.6	0.0	23.6	8.3	1509.0	0.0	0.0	0.0	0.0	27311.5
EGO	12466.6	0.0	0.6	38.6	4405.9	0.0	0.0	9.7	0.0	16921.5
GTO	769.2	0.0	0.0	8.8	5238.6	0.0	0.0	627.6	0.0	6644.3
NSO	3196.2	0.0	0.0	0.8	1973.3	0.0	0.0	0.0	0.0	5170.4
MEO	1128.1	0.0	0.0	11.2	478.7	0.0	0.0	21.6	0.0	1639.6
LMO	727.4	0.0	0.0	22.7	5483.4	0.6	0.0	1520.8	12.1	7767.0
MGO	925.1	0.0	0.0	14.7	3179.5	0.0	0.0	0.0	0.0	4119.2
HEO	656.9	0.0	0.0	0.3	1402.9	0.0	0.0	0.0	0.0	2060.0
Other	475.0	0.0	0.0	0.4	182.6	0.0	0.0	0.0	0.0	657.9
Total	211657.7	0.0	24.2	144.9	34777.2	1.9	0.0	2438.0	12.1	249056.1

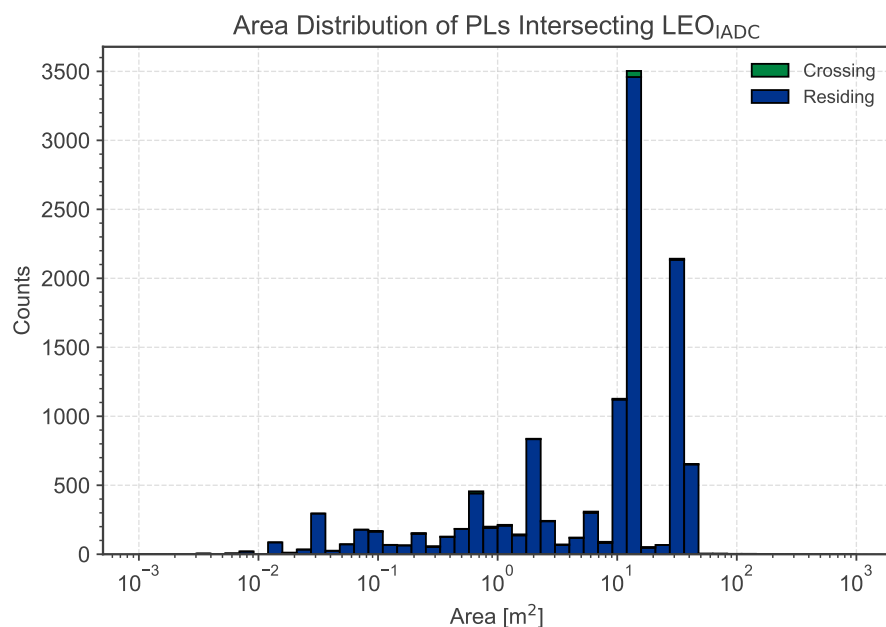
Table 3.6: Absolute and equivalent area in m^2 intersecting with the protected regions.

	PL	PF	PD	PM	RB	RF	RD	RM	UI	Total
both (abs)	237.7	0.0	0.0	0.1	1944.4	0.0	0.0	215.8	0.0	2398.2
LEO_{IADC} (abs)	167227.5	0.0	0.0	70.7	22832.5	1.9	0.0	2406.7	12.1	192551.5
LEO_{IADC} (eqv)	165733.9	0.0	0.0	45.8	11779.6	1.4	0.0	460.3	2.2	178023.3
GEO_{IADC} (abs)	29232.2	0.0	23.6	49.3	6587.1	0.0	0.0	216.5	0.0	36108.7
GEO_{IADC} (eqv)	26836.8	0.0	23.6	17.8	2279.2	0.0	0.0	17.5	0.0	29175.0
none (abs)	15435.7	0.0	0.6	25.0	7302.0	0.0	0.0	30.7	0.0	22794.0

3.1. Status of the Environment in LEO



(a) Mass histogram of payloads in LEO.



(b) Area histogram of payloads in LEO.

Figure 3.1: Distribution of mass and area of payloads in LEO.

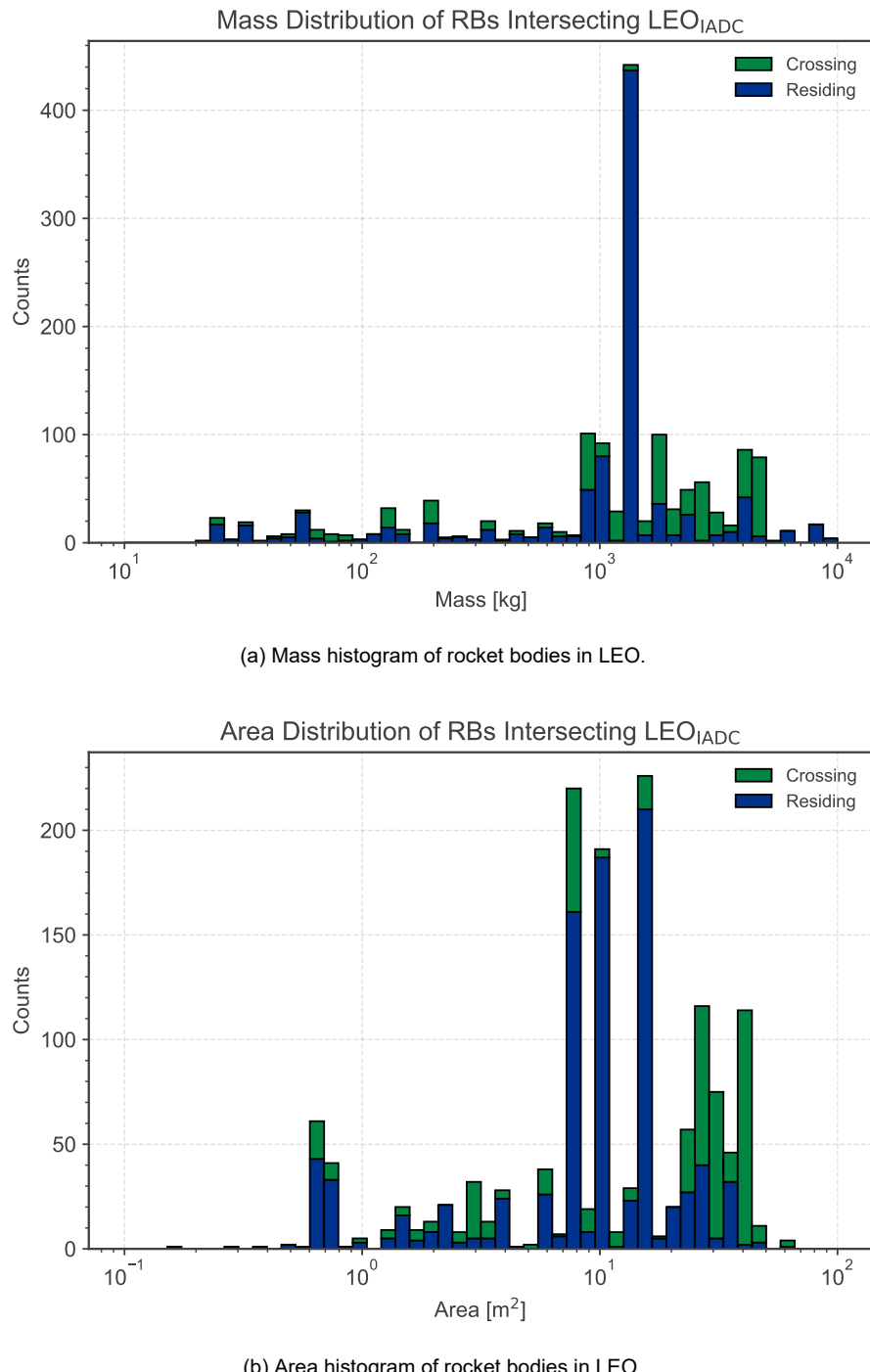


Figure 3.2: Distribution of mass and area of rocket bodies in LEO.

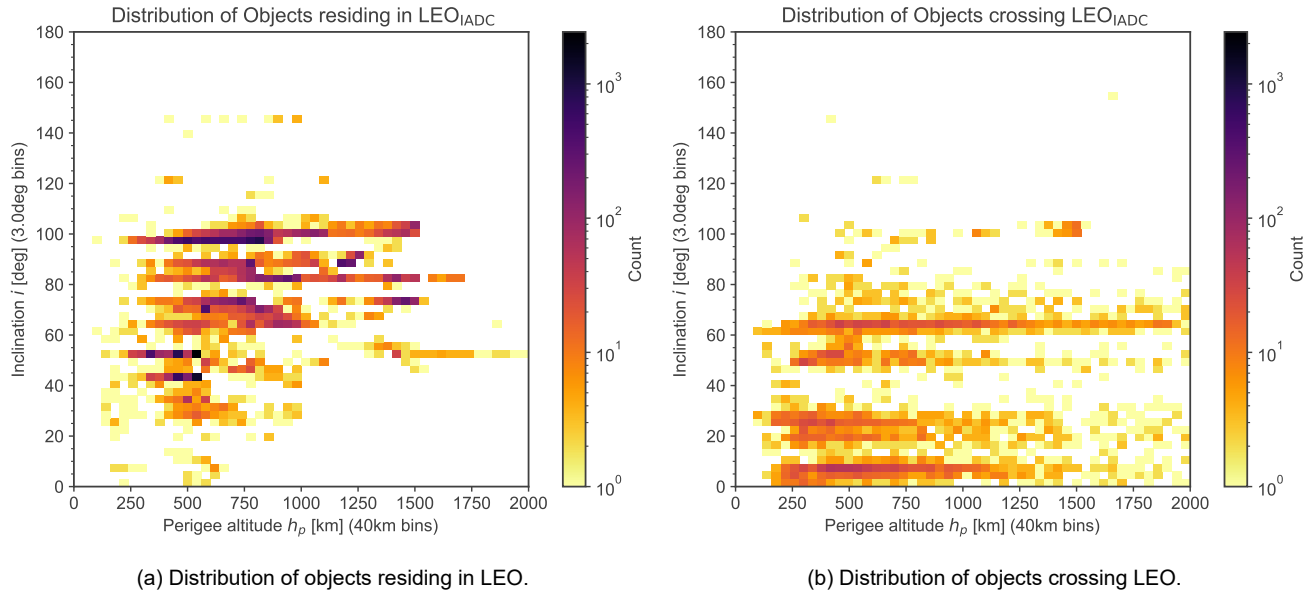


Figure 3.3: Distribution of number of objects in LEO as a function of inclination and perigee altitude.

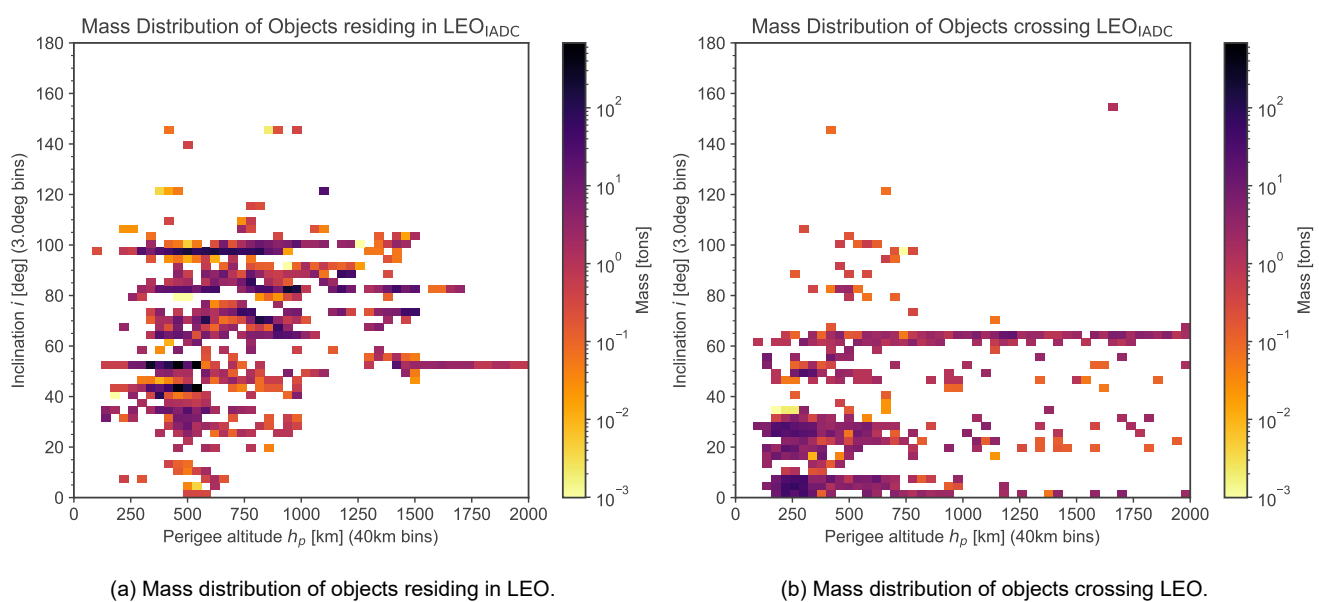


Figure 3.4: Distribution of mass in LEO as a function of inclination and perigee altitude.

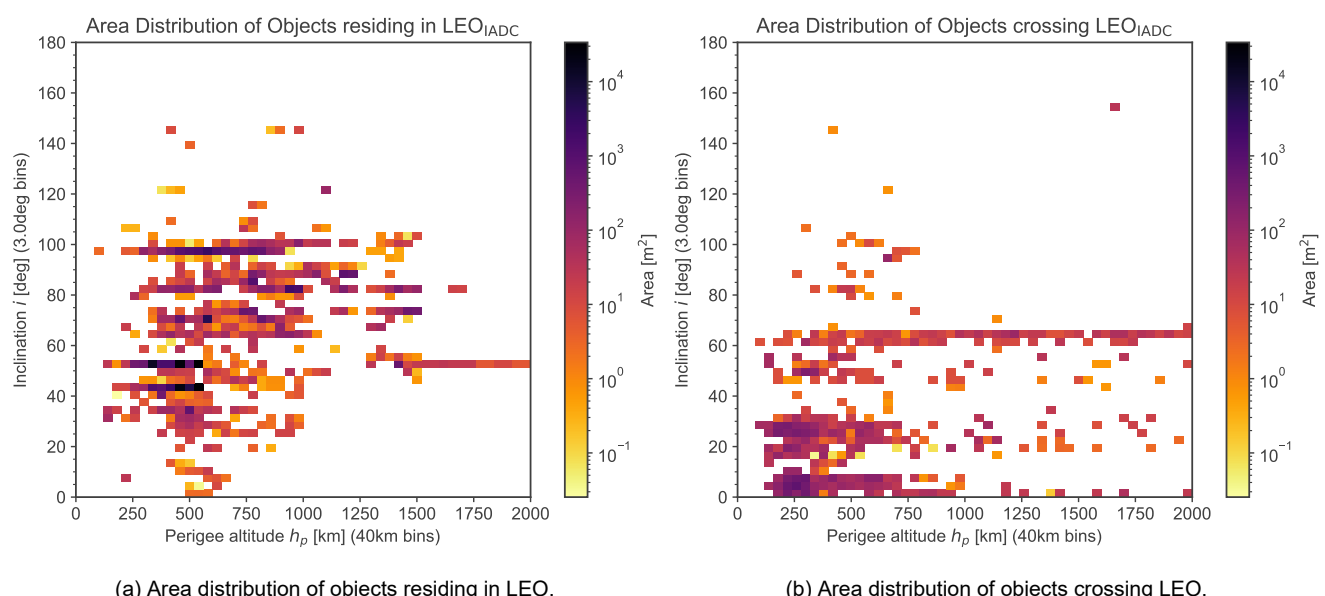
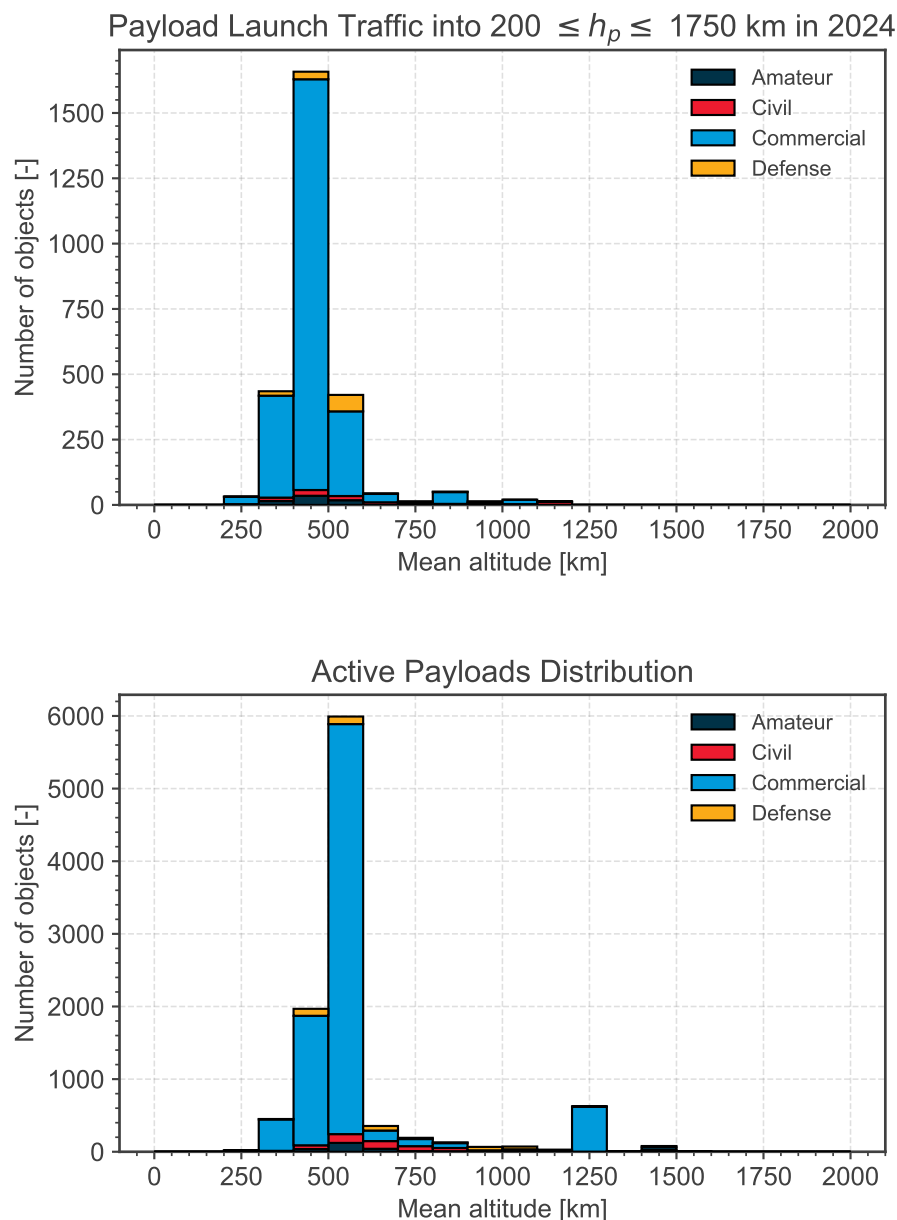


Figure 3.5: Distribution of area in LEO as a function of inclination and perigee altitude.

Figure 3.6: Launch traffic in 2024 (top) and distribution of active payloads (bottom) in LEO_{IADC} by mean altitude.

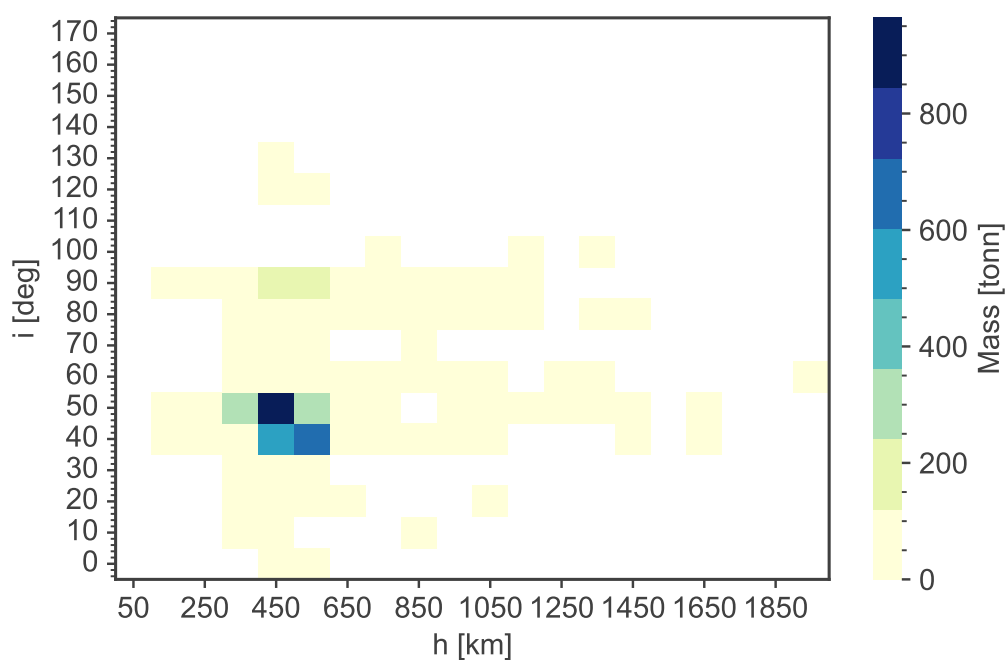
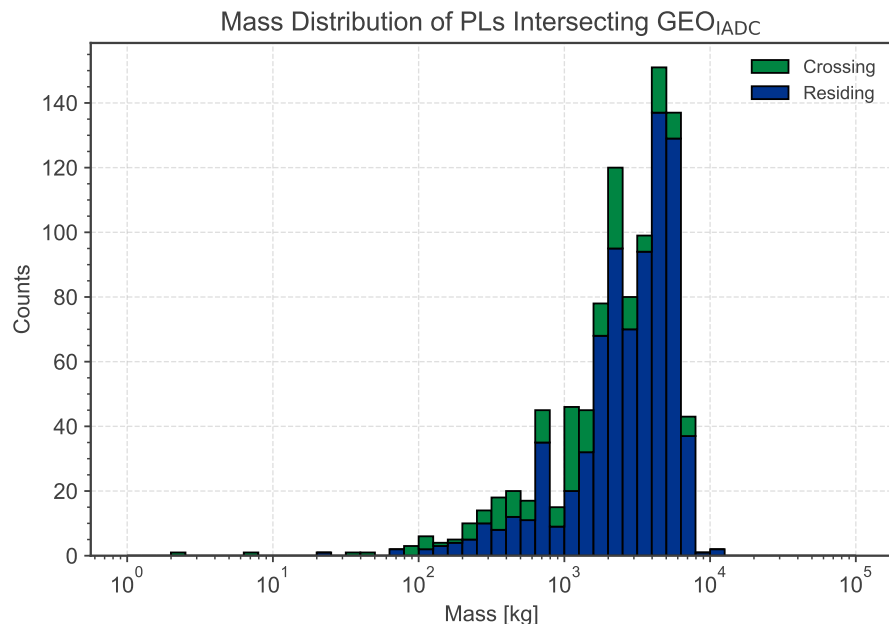
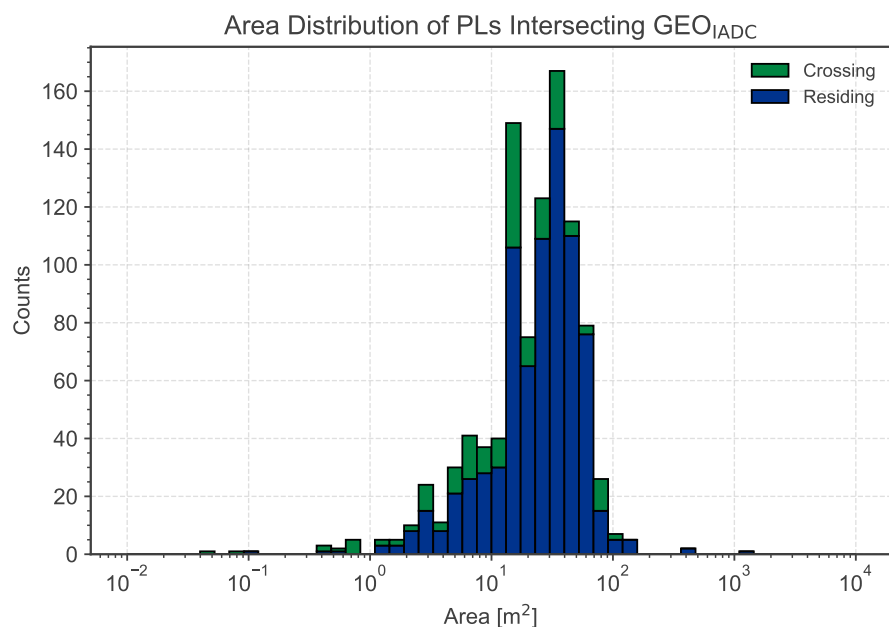


Figure 3.7: Distribution of active payloads in LEO by mean altitude and inclination.

3.2. Status of the Environment in GEO



(a) Mass histogram of payloads in GEO.



(b) Area histogram of payloads in GEO.

Figure 3.8: Distribution of mass and area of payloads in GEO.

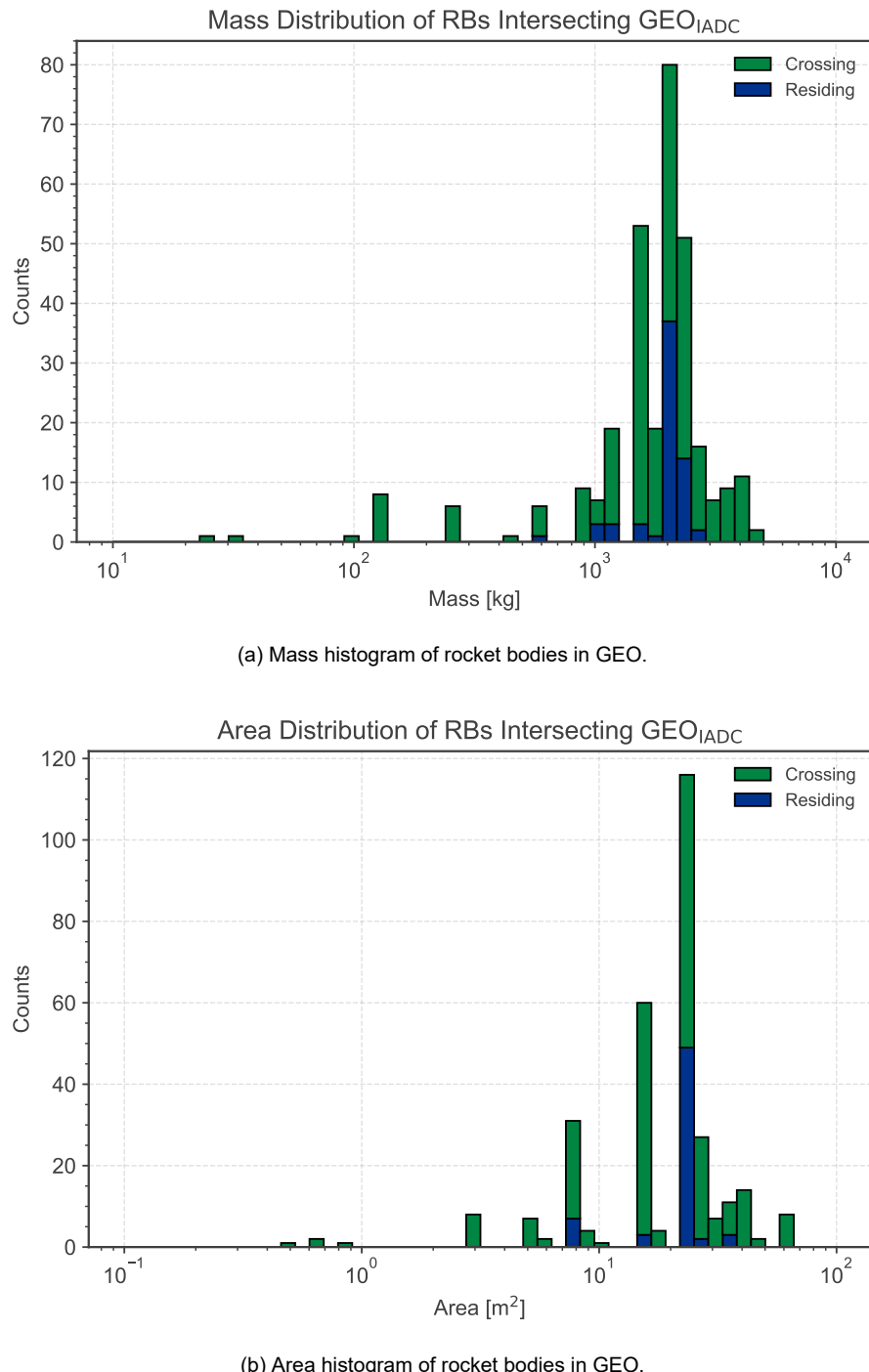


Figure 3.9: Distribution of mass and area of rocket bodies in GEO.

3.3. Fragmentations in 2024

In Table 3.7 all established fragmentation events of the year 2024 are shown. For a description of the event categories, please consult Section 5. In case no credible source is available on the amount of Asserted Objects associated with a fragmentation event, it is indicated with None. Those Asserted Object are reported by space surveillance networks which can have variable detection limits. A more in-depth overview of the consequences of those events can be accessed online [17].

Table 3.7: Fragmentation events in 2024.

Event epoch	Object type	Mass [kg]	Catalogued objects	Asserted objects	Orbit	Event cause
2024-04-02	Rocket Body	6000	0	60	LEO	Propulsion
2024-04-08	Payload	2382	0	92	LMO	Propulsion
2024-05-27	Payload	2500	0	1	GEO	Unknown
2024-06-26	Payload	5691	19	100	LEO	Unknown
2024-07-05	Rocket Body	6000	0	44	LEO	Propulsion
2024-07-19	Payload	816	4	5	LEO	Unknown
2024-08-06	Rocket Body	6000	663	700	LEO	Propulsion
2024-09-06	Rocket Body	2020	843		MGO	Propulsion
2024-10-19	Payload	2946	1104		GEO	Propulsion
2024-12-01	Rocket Body	6000	0	100	LEO	Unknown
2024-12-19	Payload	816	0	50	LEO	Unknown
Total		41170	2633			

3.4. Changes to the Environment in 2024

In this section, the change to the environment during 2024 is listed. The last state of the year is used to classify the object orbit. If no state is available, a destination orbit defined by an analyst is used instead.

Table 3.8: Number of newly added objects orbiting Earth. Other: IGO, GHO, HAO, UFO, ESO.

	PL	PF	PD	PM	RB	RF	RD	RM	UI	Total
LEO	2605	18	5	9	97	663	12	15	46	3470
GEO	20	32	0	0	0	0	0	0	8	60
EGO	1	790	0	0	2	11	1	1	423	1229
GTO	1	0	0	0	7	1	0	0	88	97
NSO	8	0	0	0	3	0	0	0	10	21
MEO	2	0	0	0	1	64	0	0	138	205
LMO	1	0	0	0	9	202	0	0	245	457
MGO	1	14	0	0	1	783	0	0	375	1174
HEO	5	178	0	0	9	30	0	0	494	716
Other	4	12	0	0	2	1	0	0	25	44
N/A	2	1	0	0	3	0	0	0	0	6
Total	2648	1044	5	9	131	1755	13	16	1852	7473

Table 3.9: Absolute and equivalent number of newly added objects intersecting with the protected regions.

	PL	PF	PD	PM	RB	RF	RD	RM	UI	Total
both (abs)	3	25	0	0	8	3	0	0	117	156
LEO_{IADC} (abs)	2612	43	5	9	124	869	12	15	483	4172
LEO_{IADC} (eqv)	2605	18	5	9	98	688	12	15	75	3526
GEO_{IADC} (abs)	24	939	0	0	8	291	0	0	1044	2306
GEO_{IADC} (eqv)	20	167	0	0	0	12	0	0	47	247
none (abs)	15	87	0	0	7	598	1	1	442	1151

Table 3.10: Newly added mass in tons orbiting Earth. Other: IGO, GHO, HAO, UFO, ESO.

	PL	PF	PD	PM	RB	RF	RD	RM	UI	Total
LEO	1762.1	0.0	0.0	3.2	185.3	0.0	0.0	0.1	9.2	1960.0
GEO	93.9	0.0	0.0	0.0	0.0	0.0	0.0	0.0	0.0	93.9
EGO	20.0	0.0	0.0	0.0	5.5	0.0	0.0	0.0	0.0	25.5
GTO	4.0	0.0	0.0	0.0	22.9	0.0	0.0	0.0	0.0	26.9
NSO	9.0	0.0	0.0	0.0	11.3	0.0	0.0	0.0	0.0	20.3
MEO	3.4	0.0	0.0	0.0	4.3	0.0	0.0	0.0	0.0	7.7
LMO	4.4	0.0	0.0	0.0	28.9	0.0	0.0	0.0	0.0	33.2
MGO	5.0	0.0	0.0	0.0	3.2	0.0	0.0	0.0	0.0	8.2
HEO	9.2	0.0	0.0	0.0	33.6	0.0	0.0	0.0	0.0	42.8
Other	2.7	0.0	0.0	0.0	7.7	0.0	0.0	0.0	0.0	10.4
N/A	2.5	0.0	0.0	0.0	5.5	0.0	0.0	0.0	0.0	8.0
Total	1913.6	0.0	0.0	3.2	302.8	0.0	0.0	0.1	9.2	2229.0

Table 3.11: Absolute and equivalent newly added mass in tons intersecting with the protected regions.

	PL	PF	PD	PM	RB	RF	RD	RM	UI	Total
both (abs)	3.2	0.0	0.0	0.0	31.7	0.0	0.0	0.0	0.0	34.9
LEO_{IADC} (abs)	1774.2	0.0	0.0	3.2	278.4	0.0	0.0	0.1	9.2	2065.1
LEO_{IADC} (eqv)	1762.5	0.0	0.0	3.2	189.4	0.0	0.0	0.1	9.2	1964.4
GEO_{IADC} (abs)	102.1	0.0	0.0	0.0	31.7	0.0	0.0	0.0	0.0	133.8
GEO_{IADC} (eqv)	94.4	0.0	0.0	0.0	0.1	0.0	0.0	0.0	0.0	94.5
none (abs)	40.6	0.0	0.0	0.0	24.4	0.0	0.0	0.0	0.0	65.0

Table 3.12: Newly added area in m^2 orbiting Earth. Other: IGO, GHO, HAO, UFO, ESO.

	PL	PF	PD	PM	RB	RF	RD	RM	UI	Total
LEO	69478.9	0.0	0.0	29.2	1368.4	0.0	0.0	0.8	64.6	70941.9
GEO	814.0	0.0	0.0	0.0	0.0	0.0	0.0	0.0	0.0	814.0
EGO	7.9	0.0	0.0	0.0	97.2	0.0	0.0	0.0	0.0	105.1
GTO	34.1	0.0	0.0	0.0	207.1	0.0	0.0	0.0	0.0	241.2
NSO	97.9	0.0	0.0	0.0	112.7	0.0	0.0	0.0	0.0	210.6
MEO	54.8	0.0	0.0	0.0	40.0	0.0	0.0	0.0	0.0	94.8
LMO	13.6	0.0	0.0	0.0	276.2	0.0	0.0	0.0	0.0	289.8
MGO	34.1	0.0	0.0	0.0	49.8	0.0	0.0	0.0	0.0	83.9
HEO	85.2	0.0	0.0	0.0	289.5	0.0	0.0	0.0	0.0	374.6
Other	9.1	0.0	0.0	0.0	86.8	0.0	0.0	0.0	0.0	95.9
N/A	45.5	2.5	0.0	0.0	66.1	0.0	0.0	0.0	0.0	114.0
Total	70629.4	0.0	0.0	29.2	2527.6	0.0	0.0	0.8	64.6	73251.8

Table 3.13: Absolute and equivalent newly added area in m^2 intersecting with the protected regions.

	PL	PF	PD	PM	RB	RF	RD	RM	UI	Total
both (abs)	16.1	0.0	0.0	0.0	292.6	0.0	0.0	0.0	0.0	308.7
LEO_{IADC} (abs)	69548.4	0.0	0.0	29.2	2227.9	0.0	0.0	0.8	64.6	71871.0
LEO_{IADC} (eqv)	69480.7	0.0	0.0	29.2	1404.5	0.0	0.0	0.8	64.6	70979.9
GEO_{IADC} (abs)	864.2	0.0	0.0	0.0	292.6	0.0	0.0	0.0	0.0	1156.8
GEO_{IADC} (eqv)	817.6	0.0	0.0	0.0	0.8	0.0	0.0	0.0	0.0	818.4
none (abs)	233.0	0.0	0.0	0.0	299.7	0.0	0.0	0.0	0.0	532.7

Table 3.14: Number of re-entered objects. Other: IGO, GHO, HAO, UFO, ESO.

	PL	PF	PD	PM	RB	RF	RD	RM	UI	Total
LEO	1087	515	5	20	108	187	16	67	13	2018
LMO	1	0	0	1	3	6	0	1	0	12
HEO	1	0	0	0	0	0	0	0	0	1
N/A	0	0	0	0	2	0	0	0	0	2
Total	1089	515	5	21	111	193	16	68	13	2031

Table 3.15: Re-entered mass in tons. Other: IGO, GHO, HAO, UFO, ESO.

	PL	PF	PD	PM	RB	RF	RD	RM	UI	Total
LEO	237.0	0.0	0.0	12.3	218.0	0.0	0.0	5.8	9.2	482.3
LMO	1.7	0.0	0.0	0.0	9.5	0.0	0.0	0.0	0.0	11.1
HEO	1.2	0.0	0.0	0.0	0.0	0.0	0.0	0.0	0.0	1.2
N/A	0.0	0.0	0.0	0.0	8.7	0.0	0.0	0.0	0.0	8.7
Total	239.8	0.0	0.0	12.3	227.5	0.0	0.0	5.8	9.2	494.6

Table 3.16: Re-entered area in m^2 . Other: IGO, GHO, HAO, UFO, ESO.

	PL	PF	PD	PM	RB	RF	RD	RM	UI	Total
LEO	6260.2	0.0	0.0	85.9	1921.4	0.0	4.7	184.9	64.6	8521.6
LMO	12.2	0.0	0.0	0.0	88.0	0.0	0.0	0.0	0.0	100.2
HEO	31.5	0.0	0.0	0.0	0.0	0.0	0.0	0.0	0.0	31.5
N/A	0.0	0.0	0.0	0.0	105.1	0.0	0.0	0.0	0.0	105.1
Total	6304.0	0.0	0.0	85.9	2009.4	0.0	4.7	184.9	64.6	8653.4

3.5. Conjunction statistics in LEO in 2024

This section aims to provide an assessment of the short-term risk related to space debris, quantified in terms of the number of conjunctions expected in different orbital regions, distinguishing also the type of secondary object involved in the conjunction. For the purpose of this report, a *conjunction* is understood as a geometric close approach between two objects, irrespective of their activity status, triggering an operator analysis but not necessarily an avoidance manoeuvre nor implying a collision.

The first step of the analysis is to define some representative *target* (or primary) objects in the conjunctions. The physical characteristics of the objects are derived from the average parameters of active payloads in LEO_{IADC}, reported in Fig. 2.31. In particular, a mass value of 355 kg and a cross-sectional area of 6 m² were used for the analysis based on the averages for 2020 and applied also to 2024 considering the consistent trend in the properties shown in Fig. 2.31, especially when considering non-constellation payloads. For what concerns the orbital parameters of the targets, two approaches are used here. The first set of representative targets is defined by looking at the distribution of active payloads in LEO_{IADC} in semi-major axis and inclination as shown in Fig. 3.7, and a total of seven targets were defined for this analysis. The second approach is to define a set of targets in the Sun-Synchronous region; in particular, seven targets are defined to cover the region between 400 and 1000 km in altitude. In both cases, twelve values of the initial longitude of ascending nodes are considered and the results presented in the following are the mean across the simulated cases for each target.

In both cases, the trajectory of the targets is propagated for one year (from 1st January 2024 to 31st December 2024) and for each day of the year an analysis is run to detect potential conjunctions with catalogued objects, by using ESA CRASS (Collision Risk ASsessment Software) [18]. For the analysis shown here, General Perturbations (GP) data is retrieved to define the orbits of the secondary objects involved in the conjunctions [19]. The data in DISCOS is used to further characterise the secondary object, for example in terms of its size and its category. In addition to the object categories defined in Section 1.1, the following subcategories are introduced:

- *Payloads* is further distinguished in:
 - *Constellation objects*, payloads belonging to a constellation,
 - *Small satellites*, payloads with a mass smaller than 15 kg,
 - *Other Payloads*, all the other payloads.
 - Each payload category is divided into *active* and *inactive* objects. Objects are considered to be active if a communication link exists and data is collected, implying that space traffic coordination may be achieved even if the active object is not manoeuvrable.
- *Payload fragmentation debris*, four subcategories were defined to collect objects belonging to the fragmentation events with the highest number of catalogued objects.
 - *Fengyun 1C Fragmentation Debris*, objects generated by the fragmentation of [Fengyun 1C](#) (1999-25A), with mass 958.0, on the 11/01/2007 at an altitude between 843.3 and 863.3 km and inclination of 98.6 degrees.
 - *Cosmos-2251 Fragmentation Debris*, objects generated by the fragmentation of [Cosmos-2251](#) (1993-36A), with mass 892.0, on the 10/02/2009 at an altitude between 776.1 and 791.1 km and inclination of 86.4 degrees.
 - *Iridium 33 Fragmentation Debris*, objects generated by the fragmentation of [Iridium 33](#) (1997-51C), with mass 661.0, on the 10/02/2009 at an altitude between 776.2 and 779.4 km and inclination of 86.4 degrees.

- *Cosmos-1408 Fragmentation Debris*, objects generated by the fragmentation of [Cosmos-1408](#) (1982-92A), with mass 2180.4, on the 15/11/2021 at an altitude between 465.0 and 490.5 km and inclination of 82.6 degrees.
- *Other Payload fragmentation debris*, all the other payload fragmentation debris.
- *Rocket fragmentation debris*, four subcategories were defined to collect objects belonging to the fragmentation events with the highest number of catalogued objects.
 - *Centaur-5 SEC Fragmentation Debris*, objects generated by the fragmentation of [Centaur-5 SEC](#) (2018-79B), with mass 2020.0, on the 06/04/2019 at an altitude between 8526.3 and 35092.8 km and inclination of 12.0 degrees.
 - *HAPS Fragmentation Debris*, objects generated by the fragmentation of [HAPS](#) (1994-29B), with mass 96.1, on the 03/06/1996 at an altitude between 584.1 and 818.9 km and inclination of 82.0 degrees.
 - *L-15 (YF115) Fragmentation Debris*, objects generated by the fragmentation of [L-15 \(YF115\)](#) (2022-151B), with mass 6000.0, on the 12/11/2022 at an altitude between 813.5 and 847.1 km and inclination of 98.8 degrees.
 - *L-15 (YF115) Fragmentation Debris*, objects generated by the fragmentation of [L-15 \(YF115\)](#) (2024-140U), with mass 6000.0, on the 06/08/2024 at an altitude between 797.9 and 855.7 km and inclination of 89.0 degrees.
 - *Other Rocket fragmentation debris*, all the other rocket fragmentation debris.

Additional information on the fragmentation events can be found in [ESA Fragmentation Database \[17\]](#).

For each conjunction, the encounter geometry (i.e. the relative orientation of the orbits and time of closest approach) is retrieved from CRASS, whereas the computation of the collision probability is performed using Alfriend-Akella's method [\[20\]](#). The values of positional uncertainty required for the collision probability calculation are obtained with the methodology in [\[21\]](#), where the covariance for an object is dependent on its size, orbit (i.e. perigee altitude, eccentricity, inclination) and time between the assessment and the Time of Close Approach (TCA).

In the results in the following, the conjunctions are grouped in *events*, where an event is defined by a pair of primary and secondary objects and a given TCA. The number of conjunction events with collision probability above 10^{-6} within three days to TCA is shown in Fig. 3.10 and Fig. 3.11, which refer, respectively, to targets defined based on the distribution of payload objects and to targets defined along the Sun-Synchronous region. The threshold at 10^{-6} is usually well below the reaction threshold for payloads in LEO_{ADC} (i.e. the events in Fig. 3.10 and Fig. 3.11 will not all result in collision avoidance manoeuvres), but this threshold could be already representative of events where increased monitoring of the conjunction is activated.

In addition to the yearly statistics, the analysis has been systematically repeated yearly since 2015. This shows, particularly in the lower LEO_{ADC} regime, the increase of conjunction events that require coordination between active operators due to the change in space traffic, whereas higher orbits remain dominated by space debris related events.

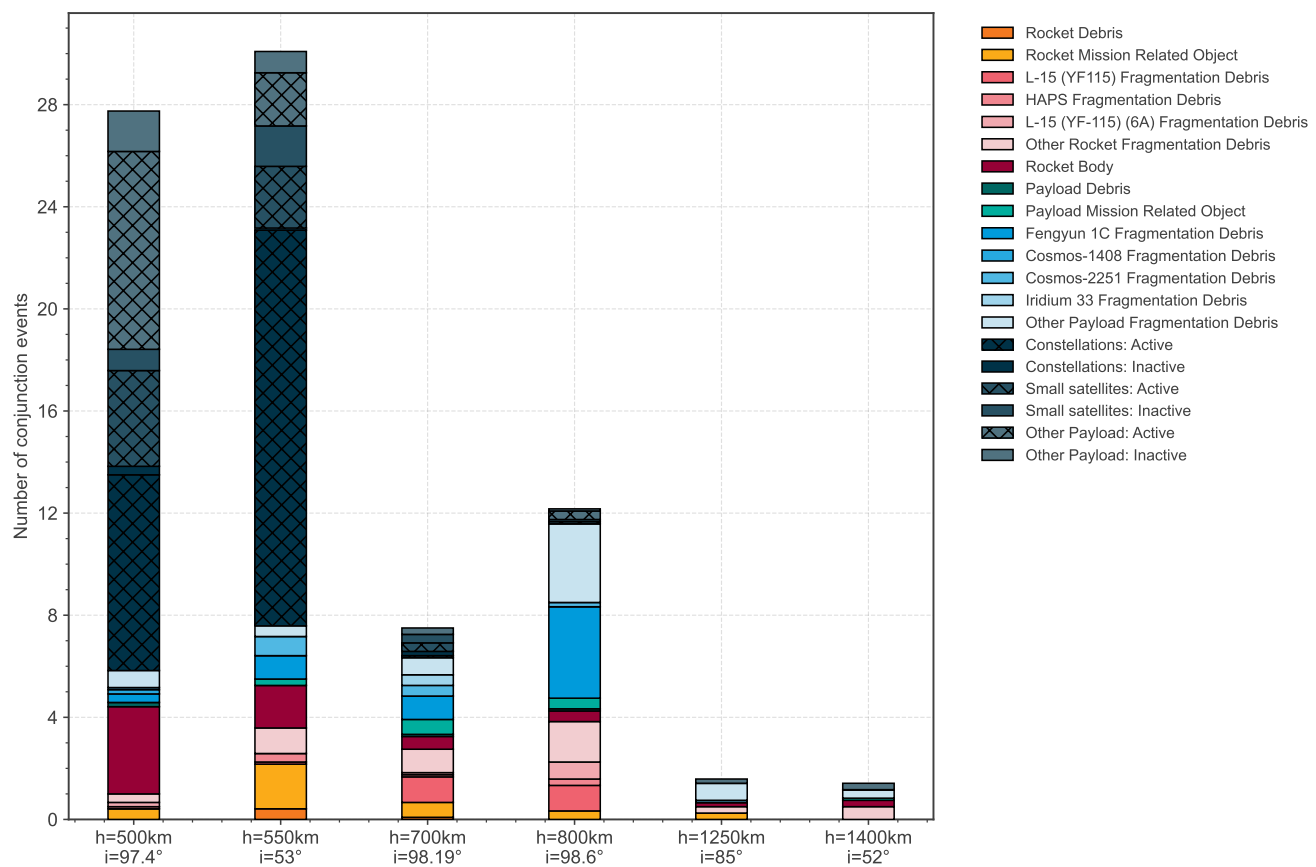


Figure 3.10: Conjunction events with collision probability above 10^{-6} , and corresponding chaser classification, for a set of representative targets over 2024.

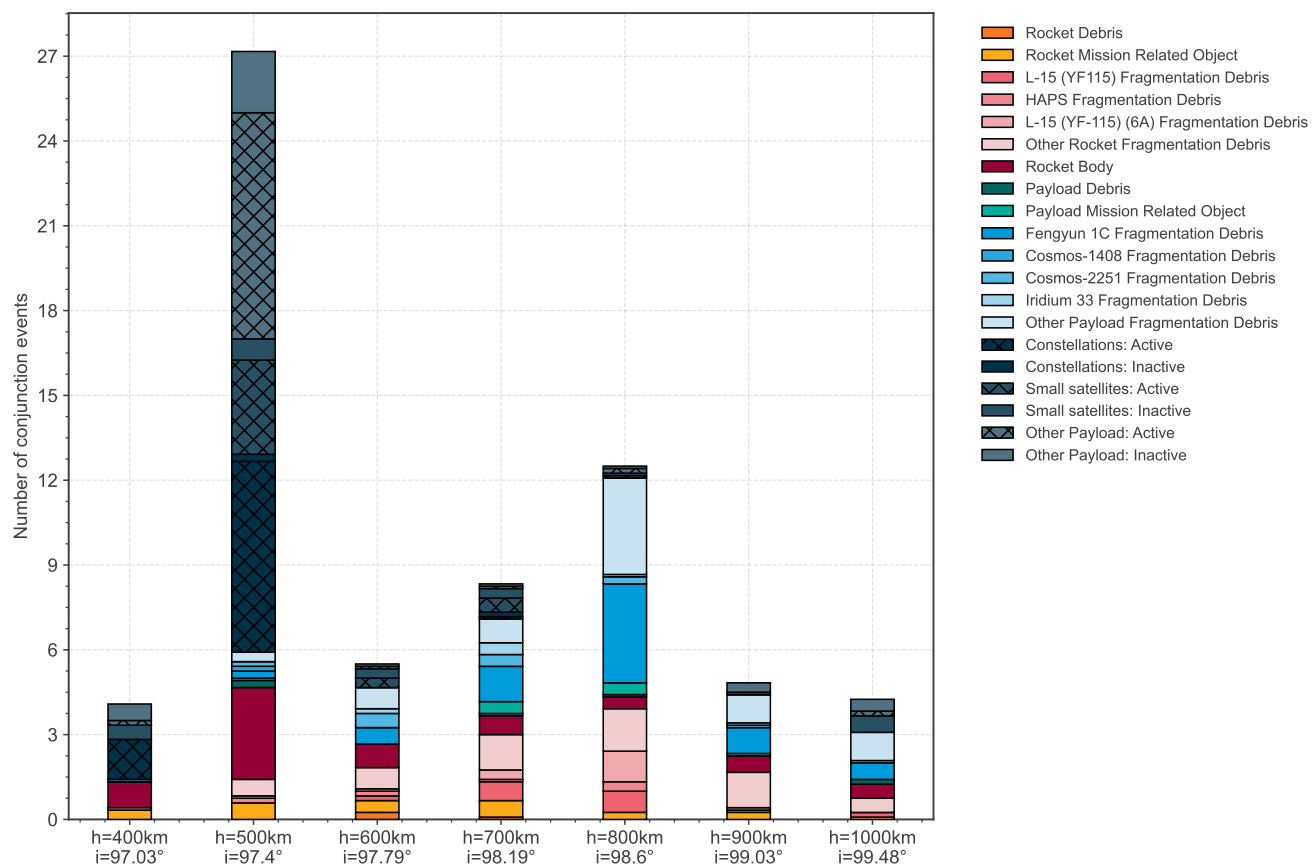


Figure 3.11: Conjunction events with collision probability above 10^{-6} , and chaser classification, for a set of representative targets in Sun-synchronous orbits over 2024.

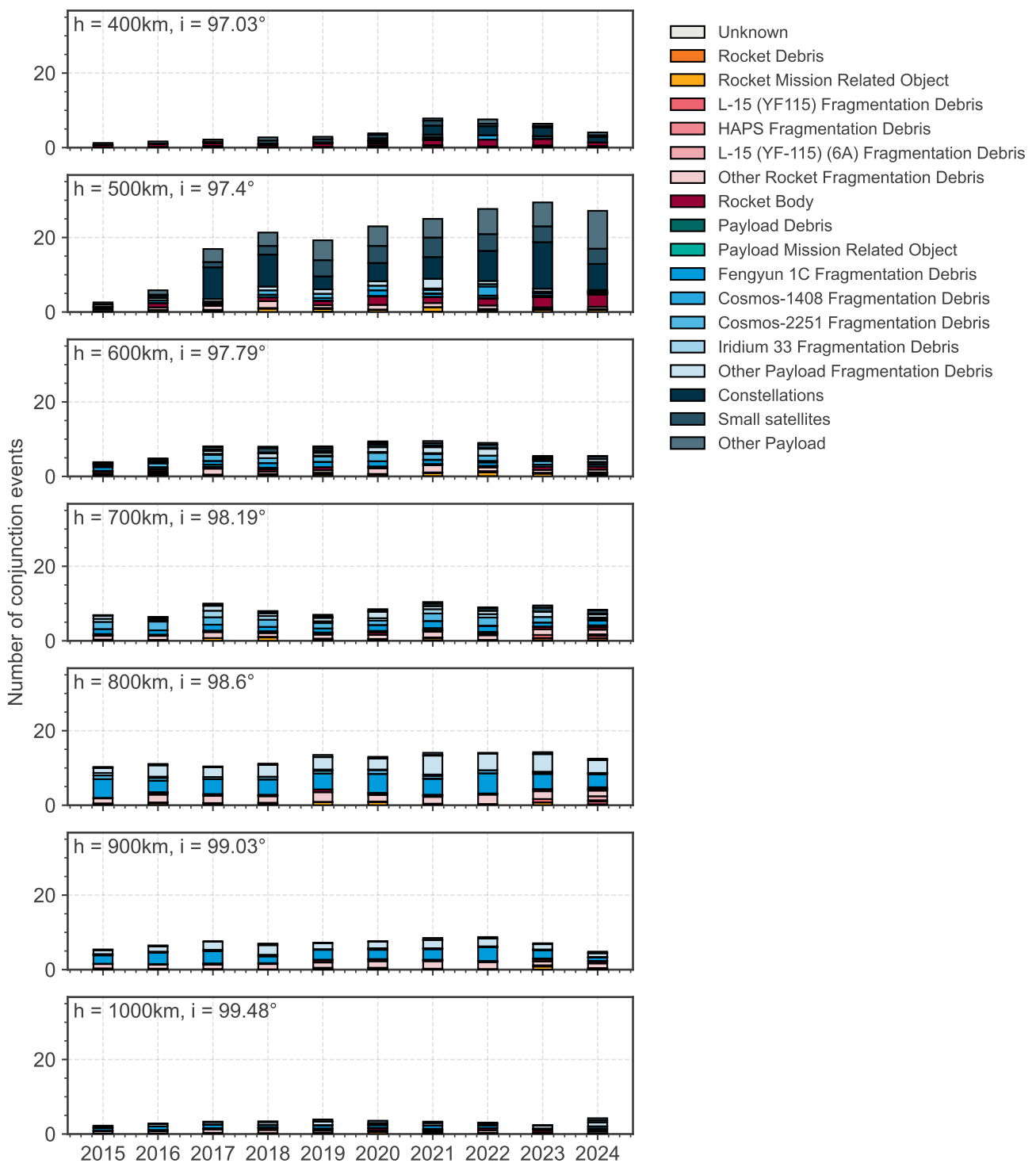


Figure 3.12: Conjunction events with collision probability above 10^{-6} , and chaser classification, for a set of representative targets in Sun-synchronous orbits over multiple years.